

OPTIMAL BINNING OF THE PRIMORDIAL POWER SPECTRUM

PANIEZ PAYKARI AND ANDREW H. JAFFE

Imperial College London
 Astrophysics Group, Blackett Laboratory, Imperial College, London SW7 2AZ, UK
Draft version October 29, 2018

ABSTRACT

The primordial power spectrum describes the initial perturbations in the Universe which eventually grew into the large-scale structure we observe today, and thereby provides an indirect probe of inflation or other structure-formation mechanisms. In this paper we will investigate the best scales the primordial power spectrum can be probed, in accordance with the knowledge about other cosmological parameters such as Ω_b , Ω_c , Ω_Λ , h and τ . The aim is to find the most informative way of measuring the primordial power spectrum at different length scales, using different types of surveys and the information they provide for the desired cosmological parameters. We will find the optimal binning of the primordial power spectrum for this purpose, by making use of the Fisher matrix formalism. We will then find a statistically orthogonal basis for a set of cosmological parameters, mentioned above, and a set of bins of the primordial power spectrum to investigate the correlation between the two sets. For this purpose we make use of principal component analysis and Hermitian square root of the Fisher matrix. The surveys used in this project are Planck and SDSS(BRG), but the formalism can easily be extended to any windowed measurements of the perturbation spectrum.

Subject headings: Cosmic microwave background — cosmological parameters — early universe — large-scale structure of universe

1. INTRODUCTION

The primordial Power Spectrum (PS) probes the physics of structure formation in the early Universe. In particular, inflation provides a paradigm for early Universe physics in accord with current cosmological observations. Simple models of inflation predict an almost Gaussian distribution of adiabatic perturbations with a scale-invariant spectrum (i.e., $P(k) \propto k$). However, there are other possibilities: for example, there could be more than one scalar field during inflation and this would predict a different spectrum and possibly a different distribution of fluctuations. The details of inflation are presently unknown to us. Therefore, determining the primordial PS would give us better intuition about the early Universe.

We use different surveys — of the Cosmic Microwave Background, of the galaxy power spectrum, of velocity fields, etc. — to constrain the primordial PS. However, the spectra of these surveys are *jointly* sensitive to cosmological parameters (which, we will collectively call θ_i) and the primordial PS. Hence there is a statistical degeneracy between the two. The aim here is to explore, as the data improve, what new information can be learnt about the primordial PS and what exactly needs to be improved to better constrain the primordial PS. The motivation is to test the assumptions about the initial conditions besides getting better constraints on parameters based on the same set of assumptions. Therefore, knowing the degeneracy between the cosmological parameters and primordial PS, we want to investigate the scales the primordial PS can be probed best with future experiments.

The outcome of different surveys is usually a type of PS that is a convolution of the primordial PS, whatever

form it may have, and (the square of) the transfer function of the particular type of survey, which holds the cosmological parameters. Here I list some examples;

- For galaxy surveys, the PS is related to the primordial PS through the matter PS, $P_\delta(k)$, as

$$P_g(k) = b^2(k)P_\delta(k) \simeq b^2(k)2\pi^2kT^2(k)\Delta_\zeta^2(k), \quad (1)$$

where Δ_ζ^2 is the primordial PS and $T(k)$ is the matter transfer function and $b(k)$ is the *bias*.

- For CMB surveys, the angular PS is

$$C_\ell = 4\pi \int_0^\infty d \ln k \Delta_\ell^2(k) \Delta_\zeta^2(k), \quad (2)$$

where ℓ is the related to the angular scale on sky via $\ell \sim 180^\circ/\theta$ and $\Delta_\ell(k)$ is the angular transfer function of the radiation anisotropies.

Here, we define the primordial curvature power spectrum, which we parameterize as $\Delta_\zeta^2(k) = A(k/0.05)^{n_s-1}$. A is the amplitude and n_s is the spectral index. The notation refers to the gauge-invariant curvature perturbation ζ (Bardeen 1980).

Other types of power spectra, such as the weak lensing and peculiar velocity power spectra, have similar forms; they depend on the cosmological parameters, through a transfer function, and the primordial PS. These different power spectra probe different scales with different accuracies. One survey can, therefore, help fill the gaps in other surveys and all together they are expected to improve information, especially on the overlapping scales. This means combining surveys can help us choose narrower bins and hence investigate the primordial PS to a greater resolution.

One common method for error estimation is to use a Fisher matrix analysis. The Fisher matrix is generally used to determine the sensitivity of a particular survey to a set of parameters and has been largely used for forecasting and optimisation. The Fisher matrix is the ensemble average of the *curvature* of a function \mathcal{F} (i.e. it is the average of the curvature over many realisations of signal and noise)

$$F_{\alpha\beta} = \langle \mathcal{F} \rangle = \left\langle -\frac{\partial^2 \ln \mathcal{L}}{\partial \theta_\alpha \partial \theta_\beta} \right\rangle \quad (3)$$

The Fisher matrix allows us to estimate the errors on parameters without having to cover the whole parameter space. Hence, the inverse of the Fisher matrix is a crude estimate of covariance matrix of the parameters, by analogy with a Gaussian distribution in the θ_a , for which this would be exact. The authors of (Bond et al. 1998) have compared the Fisher matrix analysis with the full likelihood function analysis and found there was great agreement between the two methods if the likelihood function is approximately Gaussian near the peak. The Cramer-Rao inequality states that the smallest non-marginalised error measured for the parameters by any unbiased estimator (such as the maximum likelihood) is $1/\sqrt{F}^1$. The marginalised² one-sigma error is $\sqrt{(F^{-1})_{\alpha\alpha}}$ for parameter α .

The Fisher matrix for CMB surveys is given by

$$F_{\ell\ell'} = f_{sky} \frac{2\ell + 1}{2} \delta_{\ell\ell'} [C_\ell + w^{-1} e^{\ell^2 \sigma^2}]^{-2}, \quad (4)$$

where C_ℓ is the angular PS, w is the weight defined as $(\Delta\Omega\sigma_n^2)^{-1}$ with $\Delta\Omega$ being the real space pixel size and σ_n^2 being the noise per pixel, $e^{-\ell^2\sigma^2}$ is the window function³ for a Gaussian beam (where $\sigma = \theta_{fwhm}/\sqrt{8\ln 2}$) and f_{sky} is the fraction of the sky observed. The factor $f_{sky}(2\ell + 1)$ gives the number of independent modes at a given wavenumber; the term proportional to C_ℓ is the sample (or cosmic) variance contribution, and the $w^{-1}e^{\ell^2\sigma^2}$ term is the noise contribution. Note that the diagonal form for the matrix implies diagonal (uncorrelated) errors on the C_ℓ s. To find errors on other parameters, we use the Jacobian

$$F_{\alpha\beta} = \sum_{\ell} F_{\ell\ell'} \frac{\partial C_\ell}{\partial \theta_\alpha} \frac{\partial C_{\ell'}}{\partial \theta_\beta}, \quad (5)$$

where θ_α and θ_β are different parameters.

For a volume-limited galaxy survey the Fisher matrix (Tegmark 1997) is⁴

$$F_{nn'} = \delta_{nn'} \frac{k_n^2 \Delta k V}{(2\pi)^2 (P_n + 1/\bar{n})^2}, \quad (6)$$

where V is the total volume of the survey, \bar{n} is the number density of the survey (N_{tot}/V), P_n is the galaxy PS

in each k_n bin and Δk is the binwidth. Similar to the CMB power spectrum case, $k_n^2 \Delta k V$ counts the number of modes, P_n gives the sample variance, and $1/\bar{n}$ the noise variance due to Poisson counting errors. This, again, gives us the errors on the galaxy PS and we use the Jacobian to get the errors on other parameters

$$F_{\alpha\beta} = \sum_n F_{nn'} \frac{\partial P(k_n)}{\partial \theta_\alpha} \frac{\partial P(k_{n'})}{\partial \theta_\beta}. \quad (7)$$

Fisher matrices for different surveys can easily be combined by a simple summation $\mathbf{F} = \mathbf{F}_{\text{galaxy}} + \mathbf{F}_{\text{CMB}}$. This is because they are proportional to the log of the likelihood function and we multiply likelihoods to combine them. Equivalently, we can think of them as the *weights* (inverse noise variance) of the experiments, which add for a Gaussian distribution. The nonzero correlation between the parameters in the covariance matrix makes interpreting the errors somewhat more difficult than the uncorrelated case. We will discuss various methods for decorrelating the power spectra and cosmological parameters.

2. METHOD

The aim is to investigate the primordial PS in a “non-parametric” way (we use quotations remarks to remind the reader that “non-parametric” merely means that we use a very general model, potentially with a very large number of parameters). Therefore, we assume a top-hat binning of the primordial PS

$$\Delta_\zeta^2(k) = \sum_B w_B(k) Q_B, \quad (8)$$

where Q_B is the power in each bin B and $w_B = 1$ if $k \in B$ and 0 otherwise. The cosmological parameters under investigation are (and of the form) Ω_c , Ω_b , Ω_Λ , h , τ and n_s . The reason for inclusion of n_s in the parameters is to allow for a consistency check. In this setting we do not expect to see any correlation between n_s and the bins of primordial PS. Inclusion of n_s in the parameter space only makes minute changes to our results and can be ignored. We will choose a geometrically flat (adiabatic) Λ CDM model with WMAP5 (Dunkley et al. 2008) values for the parameters; $n_s = 0.963 \pm 0.0145$ (with zero running), $\Omega_m = 0.214 \pm 0.027$, $\Omega_b = 0.044 \pm 0.003$, $\Omega_\Lambda = 0.742 \pm 0.03$, $\tau = 0.087 \pm 0.017$ and $h = 0.719 \pm 0.0265$, where $H_0 = 100 h \text{ km}^{-1} \text{ Mpc}^{-1}$. $\Omega_\nu = 0.0$ was chosen, as massive neutrinos introduce some difficulties in the Fisher matrix analysis (Eisenstein et al. 1999) and therefore were ignored for now. CMBfast software (Seljak & Zaldarriaga 1996) was used for the calculations. The surveys chosen for this initial investigation are the projected results from the SDSS Bright Red Galaxies (BRG)⁵ sample and the Planck Surveyor CMB Power Spectrum⁶.

3. GALAXY SURVEYS — SDSS (BRG)

¹ It should be noted that the Cramer-Rao inequality is a statement about the so-called “Frequentist” confidence intervals and is not strictly applicable to “Bayesian” errors.

² Integration of the joint probability over other parameters.

³ This damps power on larger ℓ s; as we get closer to the resolution limit of the survey C_ℓ s start to correlate.

⁴ Note that this equation only applies to linear regime, as nonlinearities impose non-Gaussianities.

⁵ These are bright galaxies, which means the survey can be quite deep, with $z \sim 0.25 - 0.5$. Also, these trace the elliptical galaxies, which are thought to be better tracers of mass at this redshift range.

⁶ <http://www.rssd.esa.int/SA/PLANCK/docs/Bluebook-ESA-SCI%28>

A galaxy PS is related to the matter PS via a parameter called *bias* — equation 1. For the BRG sample of SDSS, this is assumed linear and scale-independent with the form $P_g = b^2 P_\delta$, where b is the bias and approximately equal to 2.0 (Mann et al. 1998; Scherrer & Weinberg 1998; Hütsi 2006; Seljak & Warren 2004). The survey specifications for BRG sample are $\bar{n} = 10^5/V$ and $V = (1h^{-1}\text{Gpc})^3$ (Gunn & Weinberg 1995).

For the θ_i the derivatives in the Jacobian were obtained numerically using the Taylor expansion

$$P(\theta_i) = P(\theta_0) + \left(\frac{\partial P}{\partial \theta_i}\right)\Delta(\theta_i). \quad (9)$$

The width and direction of the step are quite important here. A two-sided derivative was chosen, so that the derivative is centred on the default value θ_0 , with a step size of $\Delta(\theta_i)/2$ on each side. This is accurate to 2^{nd} order in $\Delta(\theta_i)$ (a one-sided derivative would be at a slightly shifted place of $\theta_i + \Delta(\theta_i)/2$, and is only accurate to 1^{st} order (Eisenstein et al. 1999)). The width of the step should be small enough to give accurate results and yet big enough to avoid numerical difficulties. This was taken to be a 5% variation, therefore a 2.5% width on each side. Other studies have shown that this turns out to be the best step size, giving the most accurate results (Eisenstein et al. 1999).

For the primordial PS bins, the derivative is proportional to the matter transfer function

$$\frac{\partial P_g(k)}{\partial \Delta_\zeta^2(k')} = 4 \times 2\pi^2 k T^2(k) \delta_{kk'}, \quad (10)$$

where k and k' refer to the bins. The k -range for SDSS is $0.006 \lesssim k/(h\text{Mpc}^{-1}) \lesssim 0.1$. The minimum value for the wavenumber, k_{min} , is obtained from the largest scale of the survey — $(2\pi/V^{1/3})$. Its maximum value, k_{max} , is chosen to avoid non-linearities. Simulations of a very similar flat model (Meiksin et al. 1998) suggested a k_{max} of $0.1h\text{Mpc}^{-1}$. This is also very close to the scale at which departures from linear theory was seen by Percival & White (2008).

The derivatives in the Jacobian need to be averaged into bins. Later we will explain the criteria for choosing the widths and locations of the bins.

4. CMB SURVEYS — PLANCK

One thing to note in this case is that the output of CMBfast is of the form $\mathcal{C}_\ell = [\ell(\ell+1)/2\pi]\mathcal{C}_\ell$, so the CMB Fisher matrix, equation 4, is multiplied by this factor. The specifications for Planck HFI ($\nu = 100\text{GHz}$) are $\theta_{fwhm} = 10.7' = 0.003115$ radians, $\sigma_{pix} = 1.7 \times 10^{-6}$, $w^{-1} = 0.028 \times 10^{-15}$ (Delabrouille et al. 1998). The derivatives in the Jacobian were again obtained numerically by Taylor expansion

$$\mathcal{C}_\ell(\theta_i) = \mathcal{C}_\ell(\theta_0) + \left(\frac{\partial \mathcal{C}_\ell}{\partial \theta_i}\right)\Delta(\theta_i). \quad (11)$$

The same arguments as in the SDSS case applies for the width and direction of the step here. In the case of

the primordial PS bins, the derivative becomes⁷

$$\frac{\partial \mathcal{C}_\ell}{\partial \Delta_\zeta^2(k)} = 2\ell(\ell+1) \int_{k_{min}^B}^{k_{max}^B} dk |\Delta_\ell(k)|^2. \quad (12)$$

This needs to be averaged into k bins, which will be explained later on. The chosen k -range for Planck is $0.0001 \lesssim k/(h\text{Mpc}^{-1}) \lesssim 0.1$, where k_{min} was obtained from $k_{min} = \ell_{min}/d_A = 2/d_A$, where d_A is the angular diameter distance to the surface of last scattering obtained to be $\sim 14\text{Gpc}$ (Dunkley et al. 2008).

5. SDSS & PLANCK

As explained above, to combine data from different surveys, we can add the Fisher matrices obtained for each of them. We expect to see an improvement on the errors of both the bins and cosmological parameters. Equivalently, this will enable us to have narrower bins without sacrificing Signal-to-Noise per bin.

6. OPTIMAL BINNING

As explained before, a set of primordial PS bins are part of our parameter space. In this section we will explain how these bins are chosen. For our purposes the bins need to have the same amount of contribution to the Fisher matrix which means they need to have the same S/N . We take the signal in each bin to be the amplitude of the primordial PS in that bin and the noise to be given by the inverse of the square root of the diagonal elements of the Fisher matrix. For this, we construct a signal vector, \mathbf{S} , which contains the amplitude of the primordial PS for all the bins and the values of the cosmological parameters. We weight our Fisher matrix by this vector

$$F'_{\alpha\beta} = S_\alpha F_{\alpha\beta} S_\beta, \quad (13)$$

where there is no Einstein summation. This now gives us a $(S/N)^2$ matrix, where the square root of its diagonal elements are the S/N for the bins, and the weighted errors for θ_i s. It is worth to emphasise that it is this $(S/N)^2$ Fisher matrix that will be diagonalised later on.

For the SDSS case, we start by having the maximum number of bins possible in our k -range. The usual properties of the Fourier transform imply that the scale of the survey not only determines k_{min} , but also puts a limit on our resolution: $k_{min} = (\Delta k)_{min} = (2\pi/V^{1/3})$; narrower bins would become highly correlated. Therefore, we set up a series of bins with this minimum binwidth in our k -range. We then construct a Fisher matrix for this set of bins (and θ_i s) and weight it by the signal vector, \mathbf{S} , for this set. With this binning adopted, the S/N values range from 3.7 in the first bin to 35.1 in the last bin. Knowing that the binwidths chosen are the minimum possible and that increasing binwidths will increase the S/N value, we conclude that the bin with the maximum S/N cannot be changed and hence we make other bins wide enough to reach the S/N in this bin. To obtain this optimal binning we start an iteration; smaller bins of size $\simeq (\Delta k)_{min}/6$ are combined until the S/N are equal to 15% of the maximum S/N :

$$\frac{\text{Max}(S/N) - (S/N)_i}{\text{Max}(S/N)} = 0.15, \quad (14)$$

⁷ To obtain $\Delta_\ell(k)$, CMBfast needed to be altered to give the radiation transfer functions at all ℓ s. Then, for each ℓ , this was interpolated in k .

where i refers to the bins. This gives us 8 bins with their S/N ranging 30 – 35.

For Planck, the bins are obtained so that their S/N matches that of SDSS. The reason for applying this criteria to Planck is to allow for a fair comparison between the results from SDSS and Planck. This criteria gives us a total of 23 bins for Planck.

In the case of the combined Planck and SDSS we require only that the S/N of the bins are equal to 50%. This now gives us the optimal resolution of the primordial PS we can achieve from SDSS and Planck. We have a total of 48 bins with S/N being in the vicinity of ~ 20.0 and, therefore, still comparable to the S/N values in the other cases.

It is worth reminding the reader that an alternative way to determine the binning would be to take the marginalised errors as the noise. This would be obtained by inverting the Fisher matrix in each iteration loop to get the covariance matrix, which gives the marginalised variances of the bins and θ_i s. We would then take the sub-block of this covariance matrix that refers to the bins only, and invert it to get a *marginalised* Fisher matrix for the bins. We would then feed this Fisher matrix into equation 13. However, this method could not be implemented because the SDSS Fisher matrix is not invertible; the SDSS Fisher matrix is not a positive definite matrix because it is asked to estimate too many parameters. There are a total of n data points (n galaxy PS bins) and we are asking these to predict $n + m$ parameters (n primordial PS bins and m θ_i s). Also, note that whichever of the methods presented uses the *correlated* errors as the noise. We now discuss the decorrelation of the parameters.

7. DECORRELATING THE PARAMETERS

7.1. Principal Component Analysis

One popular method to overcome the correlation between the parameters is to perform principal component analysis (PCA); the covariance matrix is a symmetric $n \times n$ matrix and therefore, can be diagonalised using its eigenvectors. This has the form $\mathbf{C} = \mathbf{E}^T \mathbf{\Lambda} \mathbf{E}$, where \mathbf{C} is the covariance matrix, \mathbf{E} is an orthogonal matrix with the eigenvectors of \mathbf{C} as its rows and $\mathbf{\Lambda}$ is the diagonal matrix with the eigenvalues of \mathbf{C} as its diagonal elements⁸. This constructs a new set of variables \mathbf{X} that are orthogonal to each other and are a linear combination of the old parameters \mathbf{O} , through the eigenvectors

$$\mathbf{X} = \mathbf{E} \mathbf{O}. \quad (15)$$

The X_i are called the principal components of the experiment and are ordered so that X_1 and X_n are the best and worst measured components respectively. In this construction, the eigenvalues are the variances of the new parameters so that X_1 has the smallest eigenvalue and X_n has the largest one. The eigenvectors have been normalised so that $\sum_j e_j^2 = 1$, where e_j s are the elements of E_i . We list some properties of PCA below;

- The main point of PCA is to assess the degeneracies amongst the parameters that are not resolved

⁸ It is common to construct the covariance matrix for the PCA. However, Fisher matrix can be used instead; eigenvectors stay the same, but eigenvalues are inversed.

by the experiments, be they fundamental like the cosmic variance or due to the noise and coverage of the experiment. In our case, it will especially help us to see the correlation amongst the bins of the primordial PS, and between the bins and the cosmological parameters.

- The eigenvalues obtained measure the performance of the experiment — a larger number of small eigenvalues means a better experiment. Another measure of the performance of the experiments is to see how they mix physically independent parameters such as, say, n_s , the spectral index, and Ω_b . This sort of mixture may be improved by improving the experiment.⁹

All the above points may be summed up to conclude that in a perfect setting we would expect a one-to-one relation between the old and the new parameters. This means that we would see only one of the old parameters to contribute completely to one of the new parameters, with zero contribution from the other old parameters.

Note that the principal components obtained are not unique and depend on the form of the variables (e.g., whether we use Ω_b or $\log \Omega_b$), as well as where they are evaluated.

7.2. Hermitian Square Root

Another approach to remove the correlations between the uncertainties is to use the Hermitian square root of the Fisher matrix as a linear transformation on the parameter space (Bond et al. 1998; Hamilton 1997a,b). This transformation matrix is obtained by

$$\mathbf{F}^{1/2} = \mathbf{E}^T \mathbf{\Lambda}^{1/2} \mathbf{E}, \quad (16)$$

where, like before, \mathbf{E} is the eigenvector matrix and $\mathbf{\Lambda}$ is a diagonal matrix containing the eigenvalues. It has the property $\mathbf{F} = \mathbf{F}^{1/2} \mathbf{F}^{1/2} = (\mathbf{F}^{1/2})^T \mathbf{F}^{1/2}$ and therefore the condition $(\mathbf{F}^{-1/2}) \mathbf{F} (\mathbf{F}^{-1/2}) = (\mathbf{F}^{-1/2})^T \mathbf{F} (\mathbf{F}^{-1/2}) = \text{diag}$ is satisfied. Unlike PCA, $\mathbf{F}^{1/2}$ does not give us an orthogonal basis and instead, it can be thought of as 'window functions' for the primordial PS. We define a window matrix by

$$H_{nm} = \frac{(F^{1/2})_{nm}}{\sum_n (F^{1/2})_{nm}}, \quad (17)$$

which satisfies the normalisation condition $\sum_n H_{nm} = 1$. Hence the windowed PS is defined as

$$\tilde{P}_m = \sum_n H_{nm} P(k_n), \quad (18)$$

where $P(k_n)$ is the original primordial PS. Note that this windowed PS is not a physically motivated PS and it is just constructed for a visual presentation and understanding of the underlying correlations. However, in a perfect setting we would expect this windowed PS to be

⁹ However, the so-called 'geometrical degeneracy' (Zaldarriaga et al. 1997; Efstathiou & Bond 1999) will not be improved by improving the experiments; two models with same primordial PS, the same matter content, and the same comoving distance to the surface of last scattering produce identical CMB PS.

equal to the primordial PS (i.e., with each window function comprising a single bin).

We obtain this window matrix for the marginalised Fisher matrix of the bins and hence it can only be applied to the Fisher matrices of Planck and the combination of Planck and SDSS, which are invertible.

8. RESULTS

8.1. PCA

First we show the results for the PCA. Principal components, the X_i s, obtained for SDSS, Planck and their combination are shown as colour-coded matrix plots; X_i s are shown from left to right with increasing errors (which is equal to $1/\Lambda_i^{1/2}$, as the eigenvalues are constructed for the Fisher matrix). Original parameters are shown vertically starting with the bins on the bottom to θ_i s on the top. For the bins, the vertical width of the box is an indication of the binwidth. Some k values for the bins are shown on the figures. We group the components depending on the X_i , showing those with values greater than 0.4; those between 0.2 and 0.4; and those below 0.2.

SDSS

The result is shown in Figure 1. There are a total of 8 bins that could be obtained to meet the S/N criteria as explained above. Together with the 6 θ_i s, we have a total of 14 original parameters and 14 principal components, X_i s. The last 6 principal components are not measured well (they have large/negative eigenvalues — Table 1). This is because, as explained before, the SDSS Fisher matrix is not a positive definite matrix; we have a total of 8 data points and this means only 8 parameters (or 8 different combinations of the parameters, i.e. X_i s) can be measured.

The best measured principal component, X_1 , has only the cosmological parameters (θ_i) contributing significantly, with h being dominant. The fact that there is more than one cosmological parameter contributing to this principal component means that SDSS can only measure a linear combination of them — a degeneracy between these parameters. X_2 measures a combination of the bins and θ_i s. Other principal components, X_3 – X_8 , measure the bins only, with no contribution from θ_i s at all, and the correlation amongst the bins is between neighbouring ones only. Intuitively, you would expect more correlation between the bins and θ_i s. Remember that the errors for the bins are related to the matter transfer function — equation 10. Therefore, you would expect that a change in θ_i s would induce a change in the matter transfer function and hence a correlation between bins and θ_i s. However, look at Figure 2 where it is showing all the derivatives that goes in the Jacobian. The derivatives with respect to θ_i s seem to scale relatively close (apart from τ where it had to be multiplied by 200). However, the derivative with respect to the primordial PS bins has to be rescaled by 10^{-8} to fit in the same range as the rest of the derivatives. This suggests that perhaps the changes in θ_i s are not large enough in this setting to have a significant effect on the matter transfer function and therefore the correlation is not that significant to show effects in the PCA. Note that the correlation between the bins shows our limits to what we can learn about the primordial PS. This correlation arises due to our lack of knowledge of the cosmological

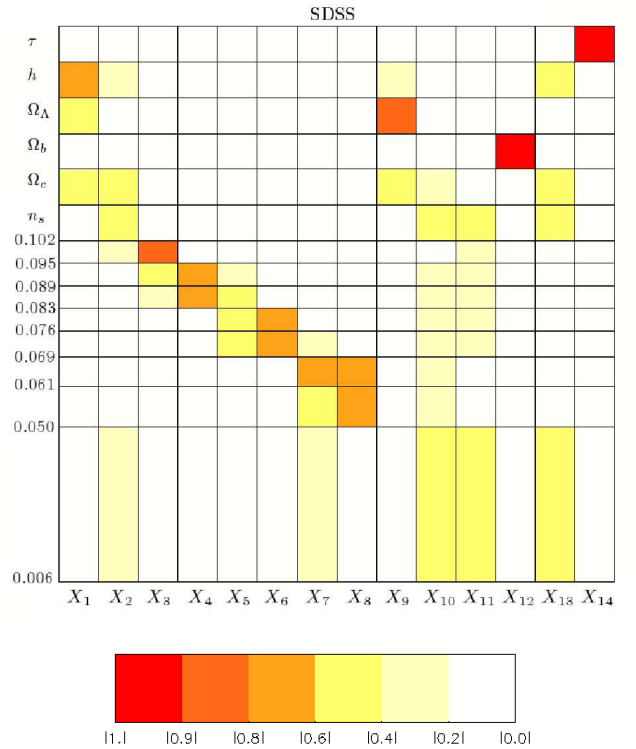


FIG. 1.— The principal components for SDSS with no priors on θ_i s. X_i are shown from left to right with increasing errors ($= 1/\sqrt{\Lambda_i}$). Original parameters are shown vertically starting with the bins on the bottom to θ_i s on the top. For the bins, the vertical width of the box is an indication of the binwidth. We group the components depending on the X_i , showing those with values greater than 0.4; those between 0.2 and 0.4; and those below 0.2. (refer to Figure ?? for the colour coding). The last 6 principal components can be ignored as they are not measured — refer to Table 1 and text for more details. At the bottom we show the colour plot indicating different levels of contribution to the principal components.

parameters. If we knew the parameters perfectly, we would have what is shown in Figure 3, which is in fact the Fisher matrix itself. Generally it seems that SDSS measures cosmological parameters better than the primordial PS and within primordial PS bins, it measures small scales better than large scales.

We also investigated what improvements we would see given better — realistic — knowledge of the cosmological parameters. Hence, WMAP5 priors (Dunkley et al. 2008) were added to constrain the θ_i s in the Fisher matrix, by adding the inverse variance of each parameter to the Fisher matrix, i.e. ignoring the correlations. The result is shown in Figure 4. Some of the degeneracies between the cosmological parameters have been broken. For example, X_2 now measures n_s almost perfectly. Also, Ω_b and τ dominate completely in X_{11} and X_{12} respectively, with no contribution from any other parameter. Note that the errors on the principal components have reduced and now all X_i s, except X_{14} , can be measured well — Table 1. This is expected as WMAP5 does a good job measuring these cosmological parameters. With respect to bins, it seems that adding priors and improving constraints on cosmological parameters has only helped to measure linear combinations of the bins better and has not been able to break the degeneracy between them.

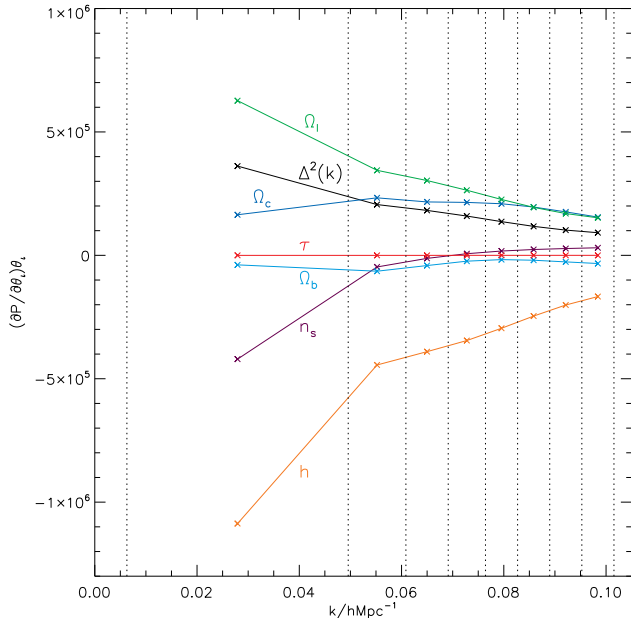


FIG. 2.— The derivative of galaxy PS with respect to the primordial PS bins and θ_i s, weighted by the parameters values. This is exactly what goes in the Jacobian. It is interesting to see in this k -range, much of the variation is on large scales. Hence it is no surprise that SDSS measures small scales better.

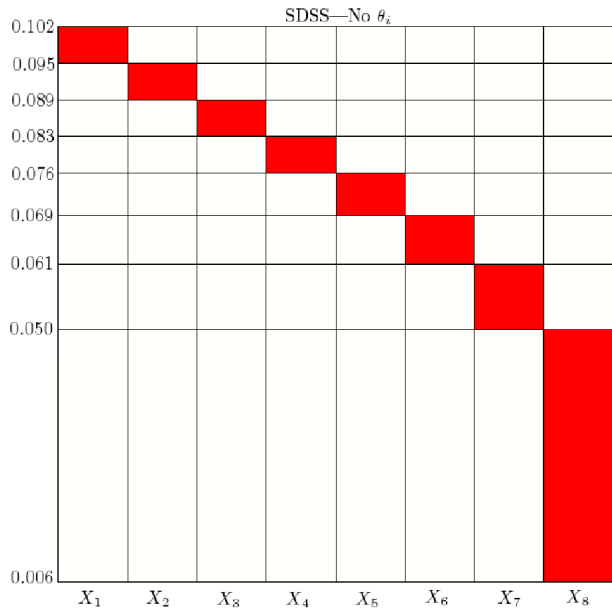


FIG. 3.— The principal components of SDSS for the primordial PS bins only, assuming θ_i s are known perfectly. No correlation exists between the bins. Compare to Figures 1 and 4, and see how the lack of knowledge of the cosmological parameters induce correlation between (neighbouring) bins.

Planck

For Planck there are a total of 23 bins and this, with the 6 θ_i s, means we have 29 principal components, shown in Figure 5. They all seem to be measured well and better than SDSS — Table 1. The reflection of the acoustic peaks of C_{ℓ} s on the bin sizes can clearly be seen; the

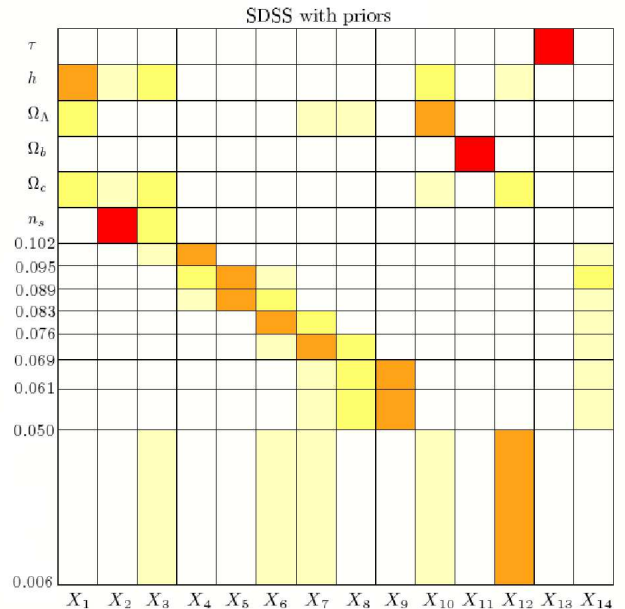


FIG. 4.— The principal components for SDSS with WMAP5 priors. Now all X_i s, apart from X_{14} , are measured well — Table 1. Also, some of the degeneracies between θ_i s have been broken.

ones corresponding to the peaks are measured with a better resolution. To see this, look at equation

$$F'_{\alpha\beta} = \sum_{\ell} [\delta_{\ell\ell'} F_{\ell\ell'}(C_{\ell})^2] \left[\frac{\partial C_{\ell}}{\partial \theta_{\alpha}} \Delta_{\zeta}^2(k_{\alpha}) \right] \left[\frac{\partial C_{\ell'}}{\partial \theta_{\beta}} \Delta_{\zeta}^2(k_{\beta}) \right], \quad (19)$$

which is $(S/N)_{\alpha\beta}^2$. This is equation 5 weighted by the signals. First bracket can be ignored as it is almost a constant due to the relation $F \propto C_l^{-2}$ — equation 4. The primordial PS, $\Delta_{\zeta}^2(k_i)$, in the second and third brackets can also be ignored as it is a constant. Therefore we are left with

$$F'_{\alpha\beta} \propto \sum_{\ell} \frac{\partial C_{\ell}}{\partial \theta_{\alpha}} \frac{\partial C_{\ell'}}{\partial \theta_{\beta}}. \quad (20)$$

For the bins the derivative in this equation is the radiation transfer function as shown in equation 12. The summation over ℓ then gives the oscillatory feature seen in k space — see Figure 6 to see the pictorial version of this.

Just like SDSS, Planck seems to measure the cosmological parameters better than the primordial PS and overall does a better job than SDSS, giving smaller errors and less correlation between them. This is not surprising as we already know Planck does a good job measuring the cosmological parameters; it measures Ω_{Λ} , h and n_s very well, with only slight correlation with other cosmological parameters. Note that n_s is measured almost perfectly with no correlation with θ_i s (or the bins, as expected).

The rest of principal components contain the highly-correlated bins only, with no particular large contribution from any of them. Intuitively one might expect the correlation to be between neighbouring bins only. The reason for the longer-range correlation lies in the form of the radiation transfer function; for each ℓ , this transfer function spans a k -range around $k = \ell/d_A$, where d_A is the

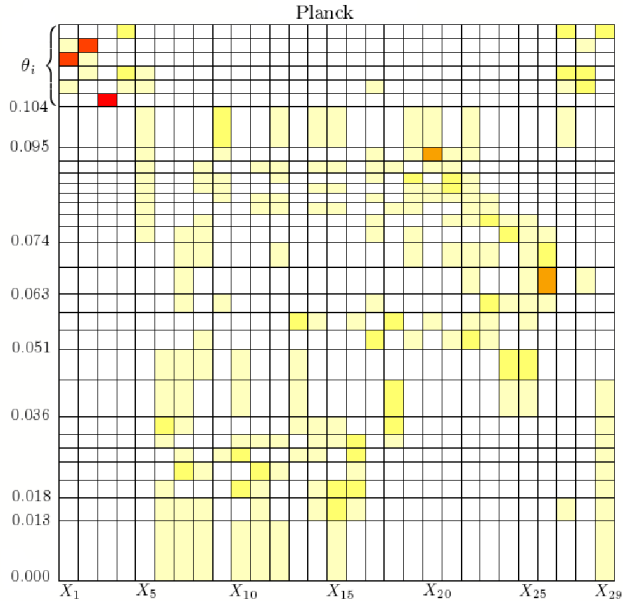


FIG. 5.— The principal components of Planck. Again bins are shown on the bottom and cosmological parameters on the top, ordered in the same way shown in previous figures. All principal components seem to be measured well and better than the SDSS case. Although, no particular scale seem to dominate strongly to any of the principal components.

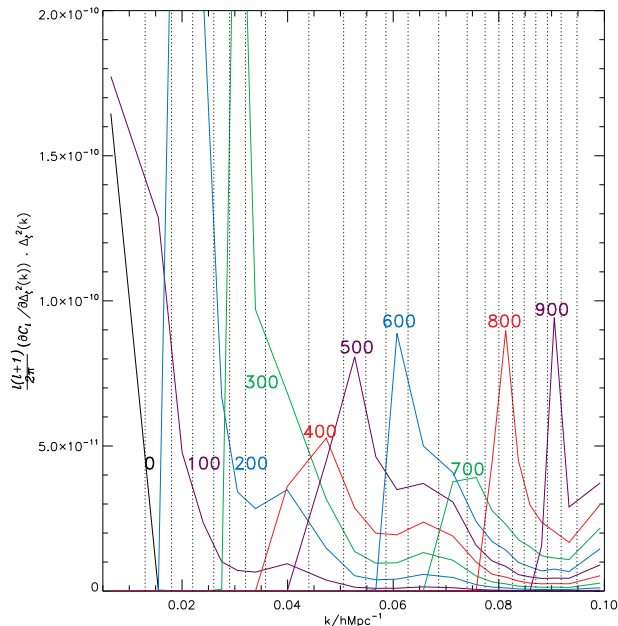


FIG. 6.— The derivative of radiation PS with respect to the primordial PS bins, equation 12, weighted by the primordial PS. Note that the bin with $\ell = 400$ dominating, gets contributions from all ℓ s from 100 to 500. This makes the correlation between the bins on all scales possible.

angular-diameter distance to the last-scattering surface. This is due to the projection of a 3D Universe onto a 2D sphere around us. Equation 12 shows what exactly contributes to the Jacobian for the Fisher matrix analysis. For each ℓ , this derivative integrates the radiation transfer function over the k -range of the bins. This would be

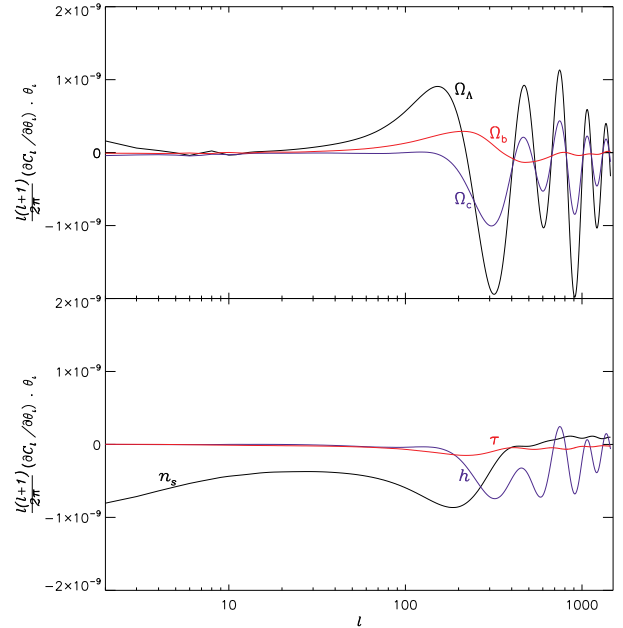


FIG. 7.— The derivative of radiation PS with respect to θ_i s. Note how different parameters dominate on different scales. For example, n_s dominates on large scales and Ω_b dominates on small scales. If Planck can only measure a linear combination of n_s and Ω_b , the degeneracy between these parameters could induce a degeneracy between large and small scale bins!

reflected as correlation between neighbouring bins. However, remember that in the Fisher matrix analysis the ℓ s get summed over (equation 5) and this now makes correlation between all bins possible; Figure 6 shows a pictorial version of equation 12, weighted by the primordial PS. Note how each ℓ spans a range of k . The summation over all ℓ s means that, for example, the bin with $\ell = 400$ dominating has contributions from all ℓ s from 100 to 500, with each spanning a different range of k . This induces correlation between bins of all scales.

This sort of correlation between small and large scales might even be worse when there is a degeneracy between the measured cosmological parameters. For example, consider an experiment that could only measure a linear combination of n_s and Ω_b , where n_s is dominant on large scales and Ω_b is dominant on small scales — Figure 7. The degeneracy between these parameters could induce a degeneracy between large and small scale bins.

We also investigated if the lack of prior knowledge of θ_i s induces extra correlation between the bins, as in the SDSS case. Figure 8 shows the principal components for the bins with no θ_i s — i.e. assuming cosmological parameters are known perfectly. Since Planck's measurements of the parameters will be much better than even those from WMAP (inclusion of which was able to remove the correlations for SDSS), we might expect little change. Indeed, not much is changed. The only improvement is on the range of errors, which now span a smaller range — Table 1. Note, however, that the smallest error for this set is still larger than the smallest error for the set including θ_i s. This is because θ_i s are generally measured better than the primordial PS bins and hence they lower the errors. Instead, comparing the largest errors of both sets shows the improvements. Despite the smaller errors

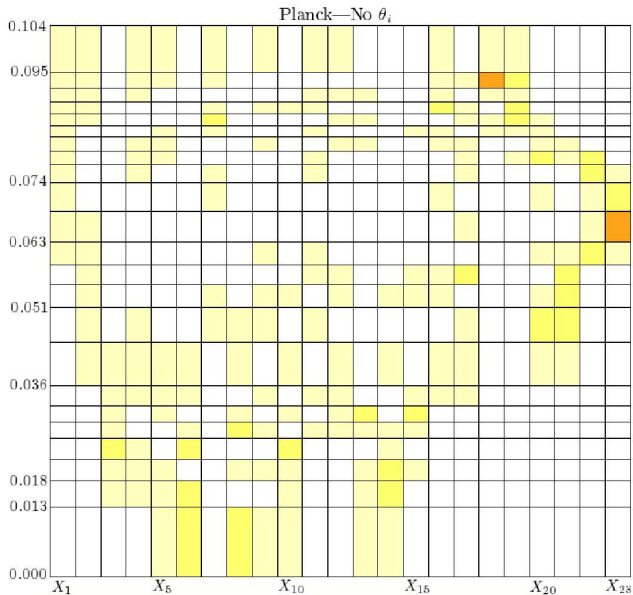


FIG. 8.— The principal components of Planck for the primordial PS bins only, assuming θ_i s are known perfectly. Compare to Figure 5. It seems like lack of knowledge of cosmological parameters does not have much of an effect in measuring the primordial PS bins in this case. This could be due to the fact that Planck measures θ_i s very well.

for this set, not much is improved in terms of correlation between the bins.

We also want to consider the bins on their own. Hence, we consider the correlation between the bins for the marginalised Fisher matrix of bins (that is, marginalised over the other cosmological parameters, θ_i s). This is obtained by inverting the parent Fisher matrix to get a covariance matrix, which holds the marginalised errors for all the parameters. Take the sub-block of this matrix which holds the errors for the bins and invert this to get a marginalised Fisher matrix and diagonalise this matrix. The principal components for this Fisher matrix are shown in Figure 9. The first thing to note is that bins contribute more significantly to some of the principal components. In particular there are some mid-scale bins which seem to be measured well. For example, look at X_{19} and X_{22} ; they seem to have uncorrelated some mid-scale bins from the rest of the bins.

Another interesting result is that very large and very small scales never really dominate in the principal components with large errors. They only contribute to them at levels of $\lesssim 0.01$. Remember that X_i s with large errors carry the most correlation and therefore the fact that mid-scale bins do not contribute to these principal components means that they are measured quite well.

To sum up, it seems like Planck will largely decorrelate the primordial PS from the θ_i s (and therefore the transfer function) but cannot exactly uncorrelate the bins themselves.

Planck & SDSS

The results are shown in Figure 10. Combining surveys has clearly helped to improve the resolution of the primordial PS. Now there are a total of 48 bins in the same k -range. Again the cosmological parameters are measured better than the primordial PS and there is also less correlation between the cosmological parameters

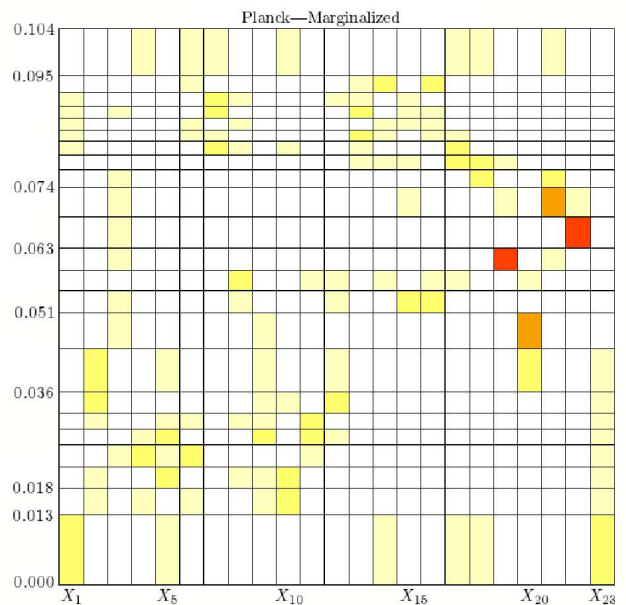


FIG. 9.— The principal components of the 'marginalised' Fisher matrix of Planck.

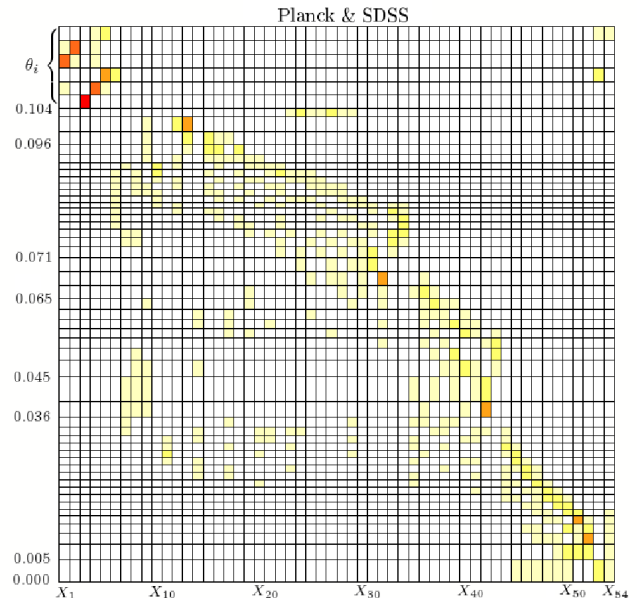


FIG. 10.— The principal components of Planck & SDSS. Clearly, resolution of the primordial PS has improved. Also, an almost diagonal trend can be seen now, showing small scales are measured better than the large scales. There is also less correlation between θ_i s.

ters compared to the previous cases. There is also less correlation between the bins themselves. Both features of SDSS and Planck can clearly be seen here. For example, acoustic oscillations in the C_ℓ s still influence the bin sizes and resolution of the primordial PS. It also seems like small scales are measured better than large scales, which is a feature seen in the SDSS case.

Figure 11 shows the results for the marginalised Fisher matrix of the bins for SDSS and Planck combined. Com-

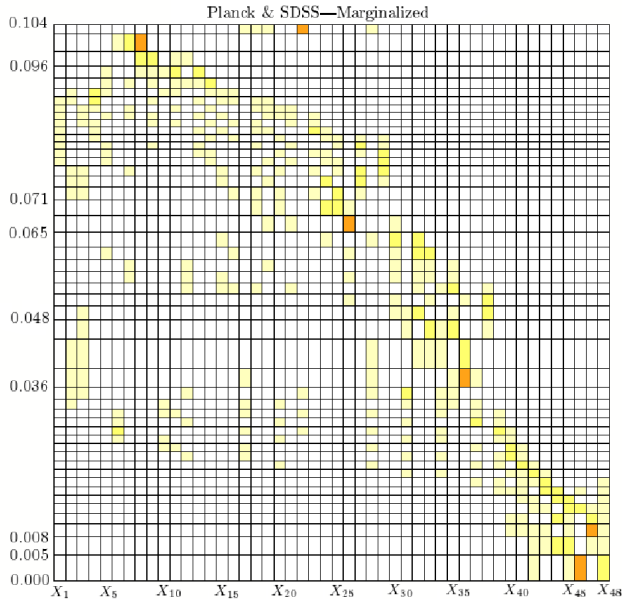


FIG. 11.— The principal components of the ‘marginalised’ Fisher matrix of Planck & SDSS.

pare to Figure 10; not much change can be seen.

8.2. Hermitian Square Root of Fisher Matrix

Figure 12 shows the window functions for Planck derived from the Hermitian square root decorrelation. Note that only the magnitude of the components of H_m s are important and not their sign. However, it is worth mentioning that for the non-marginalised Fisher matrix (both for Planck and its combination with SDSS), these window functions have only positive values. Therefore, it is the lack of knowledge of the cosmological parameters (and the induced correlation between the bins) that introduces non-physical negative values into the window functions. The window functions, H_m s, are plotted in the order of increasing errors, so that H_1 is the best measured and H_{23} the worst measured vector, respectively. Here, small scales seem to be measured best and large scales measured worst, contributing to H_m s with the lowest and highest errors respectively. It seems like Planck has not been able to decorrelate the bins completely and some correlations between *neighbouring* bins can be seen. In addition, bins in the range of $k \sim 0.02\text{--}0.04 h\text{Mpc}^{-1}$ have a large contribution to their H_m s, compared to the other bins. Compare this to Figure 13, where we diagonalised the marginalised Fisher matrix through its eigenvectors (This is exactly Figure 9 plotted in this format for easier comparison). In the PCA case, the correlations seem not to be only between neighbouring bins, but between bins of all scales, which is not seen in this case! Also, the compactness seen here (i.e. more of a window-type feature) is not seen in the PCA case; there is no particular scale that contributes significantly to the principal components.

Figure 14 shows the windowed PS for Planck. It is plotted so that each \tilde{P}_m is placed at the k_n from which it receives the largest contribution. The vertical error bars shown are $\Delta_{\zeta}^2(k_i)(\mathbf{H}\mathbf{F}^{-1}\mathbf{H}^T)$, where $\Delta_{\zeta}^2(k_i)$ is the ampli-

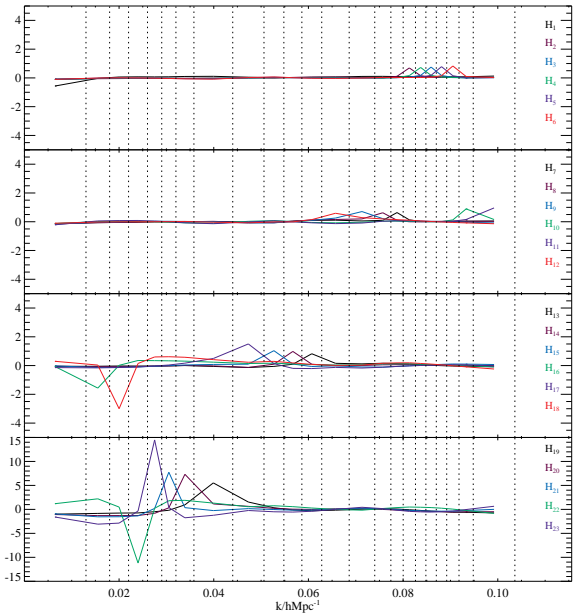


FIG. 12.— The row vectors of \mathbf{H} for the marginalised Fisher matrix of Planck. These vectors are ordered with increasing errors, so that H_1 is the best and H_{23} is the worst measured vector. This, unlike the principal components, shows that correlation is only between *neighbouring* bins and, that bins on large scales are measured better than the ones on small scales.

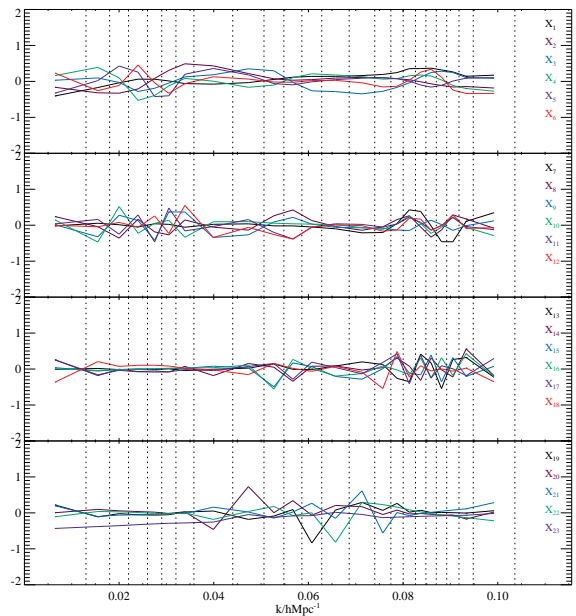


FIG. 13.— This is Figure 9 plotted in this way for easier comparison with Figure 12.

tude of the primordial PS in the bins and $(\mathbf{H}\mathbf{F}^{-1}\mathbf{H}^T)$ is the errors propagated through the H_m distribution. The horizontal error bars are the half-width at half-maximum in each direction of the main peak of each H_m . The original primordial PS is plotted for comparison. \tilde{P}_m seems to be at a lower level than the unwinded primordial PS. Remember that \tilde{P}_m is not a physical PS *per se*. How-

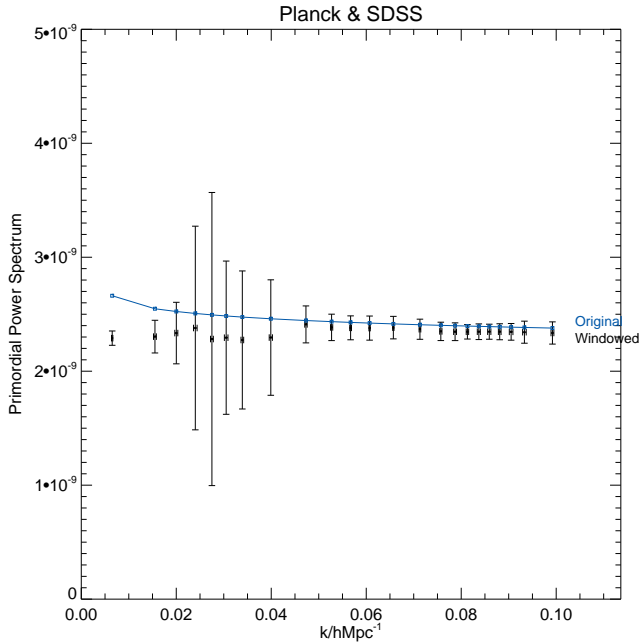


FIG. 14.— The windowed PS obtained from Planck.

ever, the observed differences from the original PS arise due to the induced correlations between the bins. In a perfect setting, where there are no correlations between bins, you do expect $\tilde{P}_m = \Delta_\zeta^2(k)$ to be true. Note that the main feature of this plot is that vertical errors, unlike those for the original primordial PS, are *not* correlated. The correlation between the errors has been transferred to overlaps between the window functions — as shown in Figure 12.

Figures 15 and 17 show the same set of results for combination of Planck and SDSS. Again large scales are contributing to H_m s with the largest errors. There seems to be less correlation between neighbouring bins compared to the Planck case. Also, note that bins in this case are narrower and therefore correlation between neighbouring bins still means correlation between a narrower range of k . Compare Figure 15 to Figure 16 (same as Figure 11). Again, there is less compactness in the PCA case, however more than what is seen for Planck on its own. Figure 15 indicates that bins in the vicinity of $k \sim 0.02 - 0.025 h\text{Mpc}^{-1}$ seem to contribute very strongly to their H_m s compared to other bins, in particular the last window function, H_{48} . This effect gets carried on to \tilde{P}_m , with \tilde{P}_{11} having a very large amplitude — Figure 17.

9. CONCLUSIONS

The primordial PS holds precious information about the physics of the early Universe and constraining it has been one of the key goals of the modern cosmology. However, the induced degeneracy between the cosmological parameters of the matter/radiation transfer functions and the primordial PS limit our ability to recover the primordial PS completely, even from a perfect survey, especially in the case of CMB surveys (Hu & Okamoto 2004). Different surveys probe different scales with different accuracies and might not be able to constrain the primordial PS to a desired resolution on their own.

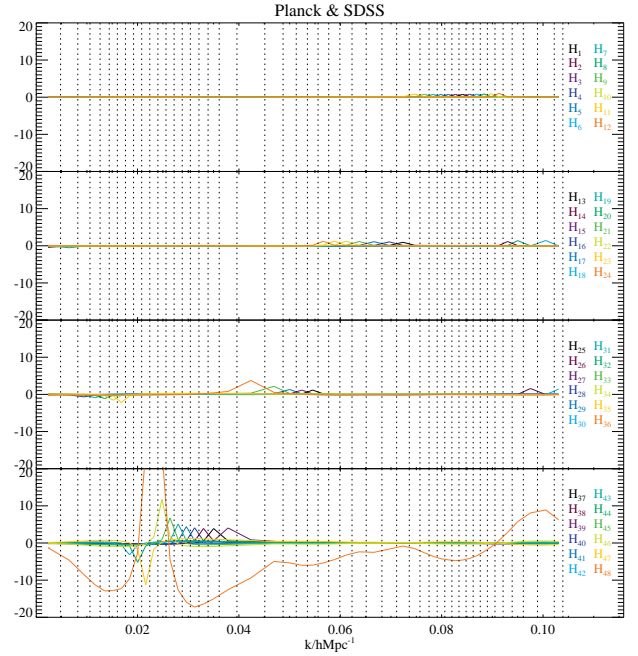


FIG. 15.— The row vectors of \mathbf{H} for the marginalised Fisher matrix of Planck & SDSS. Like before, they are ordered with increasing errors. The correlation between neighbouring bins still exists but to a lesser extent. Also, note that the bins are narrower here so that correlation between neighbouring bins still means a correlation within a narrower k -range.

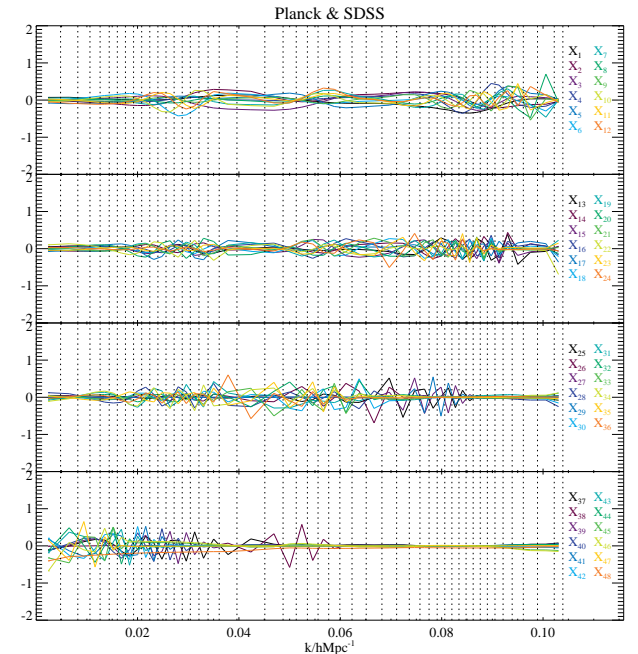


FIG. 16.— This is Figure 11 plotted in this way for easier comparison with Figure 15.

However, put together, they make significant improvements. In this paper we have investigated these limits/improvements for Planck and SDSS. For this purpose, we have assumed a non-parametric function of the primordial PS and have constructed a parameter space containing a set of *carefully chosen* bins of the primordial PS along with a set of cosmological parameters. We constructed a Fisher matrix for this parameter space for the

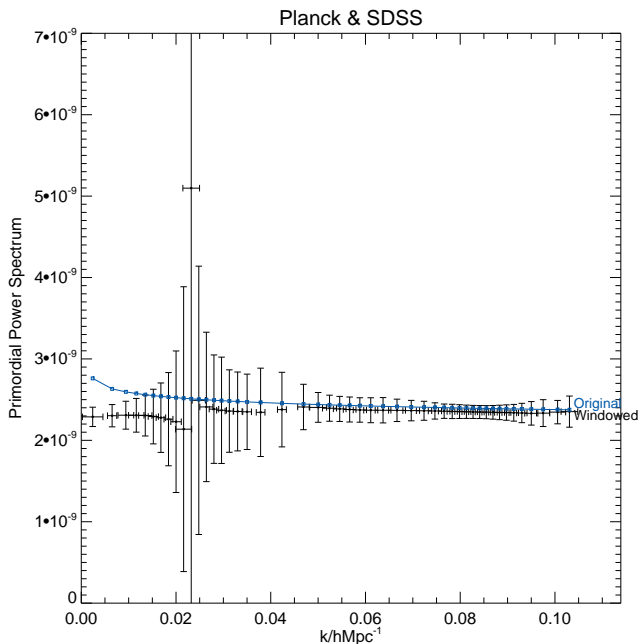


FIG. 17.— The windowed PS obtained from combination of Planck & SDSS.

two different surveys separately and combined. By diagonalising these Fisher matrices, via two different methods of eigenvector decomposition (PCA) and the Hermitian square root, we have investigated the induced correlation between the primordial PS bins and the cosmological parameters.

In the PCA case, we came to conclude that SDSS and Planck together measure the cosmological parameters to a better extent, and even break the degeneracy between them. They can increase the resolution of the primordial PS by about twice as much and can also condense the correlation between bins to be only amongst neighbouring ones. On the whole it seems like they can constrain small scales better than large scales.

By the use of Hermitian square root of the Fisher matrix we managed to divert the correlation amongst the marginalised errors of the bins to the correlation between the bins themselves. In this case, combination of SDSS and Planck helped to decrease the level of correlation between neighbouring bins, but also, because it has helped to increase the resolution of the bins, correlation between neighbouring bins means correlation between a smaller range of k .

Clearly adding the two surveys have helped to constrain the primordial PS to a better degree. Obviously, further surveys such as Ly- α (e.g. SDSS Ly α F PS), weak lensing (e.g. Euclid), peculiar velocity (e.g. Cluster Imaging Experiment (CIX)), etc. can help even more to measure the primordial PS.

We especially thank Carlo Contaldi for his great suggestions. We thank Dmitri Novikov, George Bendo, Daniel Mortlock and Gavin Nicholson for their great help. This work was supported by STFC.

TABLE 1
 ERRORS FOR DIFFERENT SETS FOR SDSS, PLANCK AND
 COMBINATION OF PLANCK AND SDSS.

SDSS	X_1	X_2	X_3	X_5	X_7	X_9	X_{11}	X_{13}	X_{14}
No priors	0.0038	0.0160	0.0287	0.0328	0.0339	7E5	NaN	NaN	NaN
No θ_i	0.0282	0.0299	0.0317	0.0340	0.0359	—	—	—	—
WMAP5 priors	0.0038	0.0123	0.0236	0.0308	0.0340	0.0357	0.0709	0.02571	23.38

Planck	X_1	X_2	X_3	X_5	X_{10}	X_{15}	X_{20}	X_{25}	$X_{28/29}$
PCA-No priors	0.0004	0.0022	0.0035	0.0152	0.0295	0.0402	0.0515	0.0700	0.4953
PCA-No θ_i s	0.0110	0.0149	0.0181	0.0224	0.0333	0.0422	0.0572	—	—
PCA-Margin.	0.0204	0.0210	0.0255	0.0313	0.0410	0.0553	0.0890	—	—
Hermitian Sqrt	0.0236	0.0261	0.0268	0.0283	0.0386	0.0487	0.2525	—	—

Planck & SDSS	X_1	X_2	X_3	X_{10}	X_{20}	X_{30}	X_{40}	X_{50}	X_{54}
PCA-No priors	0.0004	0.0020	0.0035	0.0348	0.0463	0.0548	0.0642	0.1132	0.5261
PCA-No θ_i s	0.0561	0.0568	0.0575	0.0624	0.0729	0.0891	0.1003	—	—
PCA-Margin.	0.0254	0.0289	0.0304	0.0425	0.0523	0.0598	0.0823	—	—
Hermitian Sqrt	0.0323	0.0325	0.0327	0.0374	0.0578	0.0762	0.2102	—	—

REFERENCES

- Bardeen, J. M. 1980, PRD, 22, 1882
 Bond, J. R., Jaffe, A. H., & Knox, L. 1998, PRD, 57, 2117
 Delabrouille, J., Puget, J., Gispert, R., & Lamarre, J. . 1998, ArXiv Astrophysics e-prints
 Dunkley, J., Komatsu, E., Nolta, M. R., Spergel, D. N., Larson, D., Hinshaw, G., Page, L., Bennett, C. L., Gold, B., Jarosik, N., Weiland, J. L., Halpern, M., Hill, R. S., Kogut, A., Limon, M., Meyer, S. S., Tucker, G. S., Wollack, E., & Wright, E. L. 2008, ArXiv e-prints, 803
 Efstathiou, G. & Bond, J. R. 1999, MNRAS, 304, 75
 Eisenstein, D. J., Hu, W., & Tegmark, M. 1999, APJ, 518, 2
 Gunn, J. & Weinberg, D. 1995, in Wide Field Spectroscopy and the Distant Universe, ed. S. J. Maddox & A. Aragon-Salamanca, 3–
 Hamilton, A. J. S. 1997a, MNRAS, 289, 285
 —. 1997b, MNRAS, 289, 295
 Hu, W. & Okamoto, T. 2004, PRD, 69, 043004
 Hütsi, G. 2006, AAP, 449, 891
 Mann, R. G., Peacock, J. A., & Heavens, A. F. 1998, MNRAS, 293, 209
 Meiksin, A., White, M., & Peacock, J. A. 1998, in Abstracts of the 19th Texas Symposium on Relativistic Astrophysics and Cosmology, held in Paris, France, Dec. 14-18, 1998. Eds.: J. Paul, T. Montmerle, and E. Aubourg (CEA Saclay), meeting abstract., ed. J. Paul, T. Montmerle, & E. Aubourg
 Percival, W. J. & White, M. 2008, ArXiv e-prints
 Scherrer, R. J. & Weinberg, D. H. 1998, APJ, 504, 607
 Seljak, U. & Warren, M. S. 2004, MNRAS, 355, 129
 Seljak, U. & Zaldarriaga, M. 1996, APJ, 469, 437
 Tegmark, M. 1997, Physical Review Letters, 79, 3806
 Zaldarriaga, M., Spergel, D. N., & Seljak, U. 1997, APJ, 488, 1